

An Adaptive Tracking of Weld Joints Using Active Contour Model in Arc Welding Processes

Jae Seon Kim^a, Kyoung Chul Koh^a and Hyung Suck Cho^b

^aInstitute for Manufacturing Systems Engineering, Dept. of Mechanical&Automation Engineering, Sun moon University, 100, Kalsan-ri, Tangjong-myon, Asan City, Chungnam, 336-840, Korea

E-mail: jayeekim@omega.sunmoon.ac.kr, kckoh@omega.sunmoon.ac.kr

^bDept. of Mechanical Engineering, Korea Advanced Institute of Science & Technology
373-1 Kusongdong, Yusonggu, Taejon, 305-701, Korea

E-mail : hscho@lca.kaist.ac.kr

ABSTRACT

This paper presents a vision processing scheme to automatic weld joint tracking in robotic arc welding process. Particular attention is concentrated on its robustness against various optical disturbances, such as arc glares and weld spatters radiating from the melted weld pool. Underlying the developed vision processing is a kind of model-based pattern searching, which is necessarily accompanied by two separate stages of modeling and tracking. In the modeling stage, a syntactic approach is adopted to identify unknown weld joint structure. The joint profile identified in the modeling stage is used as a starting point for successive tracking of variations in the geometry of weld joint during welding, which is automatically achieved by an active contour model technology following feature-based template matching. The performance of the developed scheme is investigated through a series of practical welding experiments.

Keywords: snakes, active contours, weld joint tracking, seam tracking, robotic arc welding, weld joint recognition

1. INTRODUCTION

Although the development of robotic arc welding systems has rapidly progressed by the continuing demand for improved methods of manufacturing industrial products, the robotization of arc welding process still suffers from several problems, such as the fixturing inaccuracies of workpiece to be welded, the workpiece-to-workpiece dimensional variations, the in-process thermal distortions, and the variations in the joint geometry. Extensive researches on the usage of visual feedback signal from the weld joint being welded have been done in order to solve these fundamental problems. However, most early vision-based robotic welding systems [1-12] have been proved still to yield several limited functionality and flexibility for the practical use. The limitations include (1) restricted use to only a few particular and simple joint types, and (2) high sensitivity to variations in the reflectance property of workpiece surface as well as welding noises, such as arc glares, welding spatters and smoke.

This paper presents a vision processing methodology with increased flexibility and robustness, which can be used for the process control as well as the torch path correction by on-line measuring the detailed geometry of the weld joint being welded. Particular interest is put on achieving the robustness against variations in the geometry of weld joint as well as various optical disturbances mainly caused by the varying reflectance properties of workpiece surface, intensive arc glares and weld spatters radiating from the melted weld pool. Underlying the developed vision processing is a kind of model-based pattern searching, which is necessarily accompanied by two separate stages of modeling and tracking. At first, the profile model of the weld joint to be welded is identified from a weld joint image with the arc turned off before the welding starts. In the second stage, tracking variations in significant features describing the weld joint geometry is done on the basis of the identified joint profile model, which is needed for consecutive correction of the torch path or the welding parameters as the welding proceeds. The vision processing with such a discriminative strategy is highly required because the vision processing during welding is in much less favorable situation than before welding on account of the effect of the unexpected brightness sources induced during welding on the weld joint image.

In our previous study [17], a sophisticated vision processing scheme with this kind of strategy has been proposed based on a syntactic analysis. However, it has been proved still not to possess the robustness enough to be severely used in practical hostile welding environment. As one of the most promising technologies to guarantee more improved robustness,

Accordingly, we advocate the usage of an active contour model with shape regulation scheme that is a modified version of “snake”, originally developed by Kass *et al.* [13] for locating a contour of interest in images. In the active contour model, a contour initially placed near the target contour of interest deforms and moves by an external potential field computed from an image data and an internal potential field caused by the prior shape constraints of the contour until the contour matches the target contour completely. The incorporation of the prior shape constraints significantly increases the robustness of the model against various disturbing noises: Typical disturbances include (1) partial occlusion of image features characterizing the target contour, (2) intrusion of some unexpected artificial image features caused by undesired illumination effect and some sensor noises induced in the image formation process, and (3) unpredictable variations in the pose and shape of the target contour. Since these kinds of disturbances frequently appear in the weld joint images obtained during welding, the active shape model is quite advantageous over other vision processing techniques frequently used for adaptive weld joint tracking, such as the least square fitting or the Hough transform following the suitable operations for stripe center detection. In this paper, a series of vision processing steps for the joint profile identification and the joint features tracking are proposed. In the joint identification stage, a syntactic approach is adopted to identify unknown weld joint structure in the absence of any detailed geometric knowledge on the weld joint. Once the joint profile is identified, the active contour is initialized by placing the core of the active contour on the resulted profile. The automatically initialized active contour model is used for successive tracking of the weld joint during welding, where the main usage of the model lies in initializing the elastic shape model and building a template characterizing the weld joint structure. The template is composed of the break points located at the significant orientation changes along the identified joint profile and it is used for detecting significant joint features from the obtained joint profile during welding. To cope with any variations in the joint geometry as the welding proceeds, the joint profile model is consecutively updated on the basis of the joint tracking results at the previous processing time. Accordingly, successive tracking of the weld joint features can be always achieved as long as the geometry and pose of the weld joint is not abruptly changed in a large amount. The rest of this paper is organized as follows. Section 2 gives an overview of the developed visual seam tracking system. Section 3 and 4 provide a full detail of the proposed vision processing algorithm for joint modeling and tracking. Section 5 gives several experimental results to demonstrate the performance of the developed methodology. Some practical seam tracking results by welding robot guided by the vision sensor are exhibited. Finally, some conclusions are made in the last section.

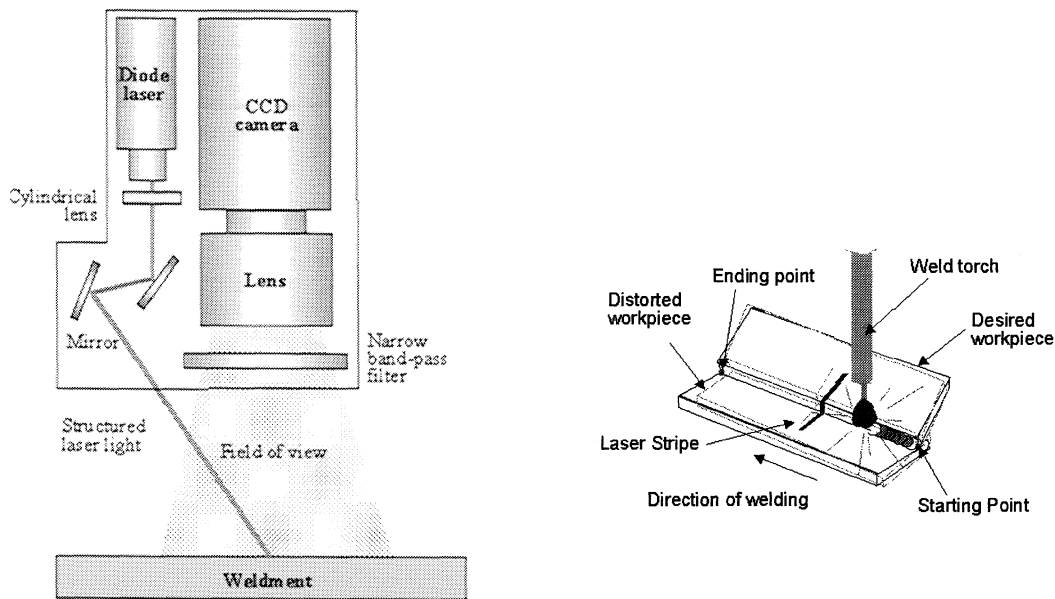


Fig. 1. Configuration of the vision sensor. Fig. 2. Arc welding system with vision-guided path correction.

2. OVERVIEW OF THE ADAPTIVE SEAM TRACKING SYSTEM

In our developed system, an articulated robot with six degrees of freedom is carrying a welding torch and a vision sensor system. The vision sensor views the weld joint ahead of the welding torch as the robot travels along the seam, as shown in Fig. 2. The images from the vision sensor are analyzed by a vision processing system, which computes the geometry of the weld joint. The processing result is sent to the control system of the welding robot in order to achieve good torch positioning or process control against any variations in workpiece geometry or position.

The developed vision sensor consists of a CCD image sensor and a compact optical projection system that generates a plane of light beam, as shown in Fig.1. The camera is fitted with a narrow-band optical interference filter having a spectral bandpass of 10nm centered at the 690nm. The narrow-band interference filter efficiently removes much of the ambient and welding arc light from the image. The optics is so arranged that one pixel in the image plane corresponds approximately to 0.05mm on a focused object. The sensor's field of view and resolution are reconfigurable depending on the application requirements. As a source of light, the 25mW laser diode emitting at 690nm is used. The visible light source with this band considerably facilitates the calibration of the sensor in the stage of development of the vision sensor. Simultaneously, it facilitates the segmentation of the laser light from the image because most significant spectral components of scattered light from the arc exist in the ultraviolet and visible bands near the ultraviolet [14]. The sensor operates on a principle of active triangulation ranging that has been used to obtain information about the 3-dimensional layout of surfaces [15]. A sheet of the laser light beam emitted through a cylindrical lens irradiates the weld joint from above and at right angles to the weld seam. To take a picture of the weld joint section, at the same time, the CCD camera looks at the irradiated joint area at a suitable angle from the beam direction. The resulting laser stripe image depicts the layout of a particular cross-section of the weld joint surface, as shown in Fig. 2.

3. JOINT IDENTIFICATION AND MODELING

The goal is to identify a generic model for the structure of the weld joint to be just welded, where the derived model is used for tracking variations in the weld joint geometry as the welding proceeds. The work is done on a weld joint image acquired around the starting point of the weld seam before the welding starts, which is free from arc light and spatters. The vision algorithm is accompanied by several consecutive steps and a detail of the methodology in each step is given in the followings.

3.1. SEGMENTATION OF JOINT PROFILE

The first step is to extract the main part of the laser stripe describing the cross-section profile of weld joint from the whole image data. The basic idea is to convolve the pixel data with a spatial filter such as the second derivative of a Gaussian that operates only in the direction of the columns of the image, because the laser stripe exhibits a hat-shaped intensity profile along the columns of the image and a greater part is posed approximately in parallel or at less angle than 30 degrees with respect to the rows of the image. However, there still remains a problem in determining the scale value of the Gaussian to easily discriminate the main part of the laser stripe from other possible brightness sources, such as arc glares and welding spatters. One of the most criteria for discriminating the laser stripe is its own thickness in the image plane. Therefore, we advocate the usage of an adaptive filter, which selectively responds to the thickness of the bright band measured along the columns of the image. Let us consider the thickness of the laser stripe L_w measured by averaging the width values of the brightest band on each of the n columns sampled in a random manner. Then, the following approximation can be used for such an adaptive filter:

$$R(i, j) = \sum_{m=-3/2L_w}^{3/2L_w} w_m I(i, j + m) \quad (1)$$

where $I(i, j)$ denotes the pixel value at the image coordinates (i, j) and w are filter coefficients. Note that the sum of the coefficients is equal to zero. For a given column i , the filter scans along the column to convolve the intensity data, and then the row of the maximum response j_{\max} is searched. If the maximum response $R(i, j_{\max})$ is larger than a threshold value, the corresponding position (i, j_{\max}) is considered to be the center of the laser stripe in the column. Once the laser stripe is extracted, the center position data are grouped into a set of connected runs. After the grouping is completed, the resulting connected runs are fitted to straight-line segments by using the polygonal line approximation method [16]. The basic idea is to find the break points located at the significant orientation changes along the connected run.

3.2. SYNTACTIC ANALYSIS

We are interested in identifying the inherent structure describing the weld joint profile. However, a series of the resulting line segments are hard to be exactly matched to the inherent joint profile on account of the presence of some unexpected parts, such as missing, artificial or overrefined ones. The goal of syntactic analysis is to revive the inherent joint structure from the degraded line segments.


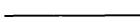




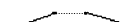

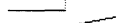

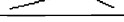



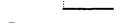
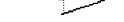
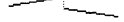



STRUCTURE LABELING

The first step for syntactic analysis is to translate the primitive joint profile into a shape-descriptive string of linguistic words. Each of line segment and junction between two neighboring line segments is assigned a label in accordance with a

pre-defined vocabulary, as shown in Table 1.

A line segment is assigned the label of "speckle" or "surface" according to its length. A threshold value D_{th} is used to discriminate between speckle and surface segment in the similar manner to the original work by Sicard *et al.* [8]. In addition, eighteen junction labels are defined to characterize the positional arrangement and the orientation change between two adjacent line segments as shown in the Table. A threshold value U_{th} is needed for deciding whether there is significant lateral gap between two adjacent line segments, and also another threshold value V_{th} is used for deciding whether there is significant upward or downward transition. Moreover, a threshold value P_{th} is used for deciding whether there is significant change in orientation between two adjacent line segments. The labeling process finally yields a string of shape-descriptive words that alternate between line segment label and junction label.

Table 1. Shape-descriptive labels

	Label	Description
Line Primitives	<i>speckle</i>	
	<i>surface</i>	
Junction Primitives	<i>cp</i>	
	<i>cu</i>	
	<i>cd</i>	
	<i>gp</i>	
	<i>gu</i>	
	<i>gd</i>	
	<i>up</i>	
	<i>uu</i>	
	<i>ud</i>	
	<i>ap</i>	
	<i>au</i>	
	<i>ad</i>	
	<i>dp</i>	
	<i>du</i>	
	<i>dd</i>	
<i>bp</i>		
<i>bu</i>		
<i>bd</i>		

STRUCTURE REFINING

The next step is to refine the expressed structure such that only some significant joint segments and junctions remain in the final representation. Starting from the leftmost three words, the string is merged and the corresponding line segments and junctions are modified according to the production rules listed in Table 2.

The rules with the expression of $A \rightarrow B$ indicate that the expression A can be replaced by the expression B . The rules falling under the second category with the expression of $A \rightarrow\rightarrow B$ replace three words of the expression A by a word of the expression B , and make a new line segment to connect between the starting point of the left line segment and the ending point of the right one in the expression A . After that, two junctions attached to each side of the newly produced line segment are relabeled. The overall meaning of this class of rules is to merge two succeeding line segments contacting each other if the change in orientation between them is small, or two speckle segments succeed each other. Exceptional cases are rules 16 and 18, which are particularly intended for eliminating some excessive speckles that are likely to be yielded around rounded off edges on workpiece.

In the rules with the expression of $A \leftarrow B$, the modification is performed according to the particular strategy in the expression B . The rules 20 and 21 are intended for removing some isolated speckles yielded by some highlighted spot on workpiece surface. The rules 22, 23 and 24 are particularly considered for enhancing the detection accuracy of joint features that may be disturbed by some unexpected tiny gaps between two significant surfaces or rounded off edges of workpiece. Such unexpected tiny gaps usually occur due to the incomplete fixturing and preparation of workpiece or its distortion during welding.

Starting with the leftmost word in the input string, each rule 1-22 is applied one after another. If a match occurs, the

modification is performed according to the matched rule. By the rules 1-22, the modification process is repeated until no more match is made over the whole string. Finally, rules 23 and 24 are in turn applied to the resulting string to enhance the detection accuracy of intersection points.

Table 2. Production rules

	Expression	
Rule 1	<u*>	→ <float>
Rule 2	<a*>	→
Rule 3	<d*>	→
Rule 4	<b*>	→
Rule 5	<float>	→ <break>
Rule 6	<g*>	→
Rule 7	<cu>	→ <vertex>
Rule 8	<cd>	→
Rule 9	<vertex>	→ <contact>
Rule 10	<cp>	→
Rule 11	<speckle>	→ <arbitrary>
Rule 12	<surface>	→
Rule 13	<speckle><contact><speckle> (if the distance between the start point of the first speckle and the end point of the second speckle does not exceed a threshold value D_m)	→→ <speckle>
Rule 14	<speckle><contact><speckle> (else if the distance exceeds a threshold value D_m)	→→ <surface>
Rule 15	<speckle><cp><surface>	→→
Rule 16	<speckle><vertex><surface> (if preceded by <break>)	→→
Rule 17	<surface><cp><speckle>	→→
Rule 18	<surface><vertex><speckle> (if followed by <break>)	→→
Rule 19	<surface><cp><surface>	→→
Rule 20	<surface><float><speckle> (if followed by <float>)	← Remove
Rule 21	<speckle><float><speckle> (if followed by <float>)	← <speckle>
Rule 22	<surface><vertex><speckle> (if followed by <vertex><surface>)	←
Rule 23	<arbitrary><vertex><arbitrary> (if the end point of the first segment is not identical to the start point of the second segment)	← Modify two neighboring segments to contact at the intersection point of the extension of the first segment and the extension of the second segment
Rule 24	<arbitrary><cp><arbitrary> (if the end point of the first segment is not identical to the start point of the second segment)	← Modify two neighboring segments to contact at the middle point between the end point of the first segment and the start point of the second segment

3.3. JOINT PROFILE MODELING

The next is to identify the structure of the weld joint. To do so, the string that survives the refining process is attempted to be matched to the pre-defined generic string models for typical weld joints. If a match is found, structural features of the weld joint are obtained from the series of the line segments matched with the generic string model. If we assume that the workpiece is composed of only flat surfaces, then inherent structure of the weld joint can be expressed by a series of branches $T = T_1 \cdot T_2 \dots T_m$, in which m is the number of the line segments, and each branch T_i has two components: the length l of the line segment and the angle θ of the line segment with respect to the rows of the image. Also, the pose of the weld joint can be expressed by a series of the image coordinate of the end points of each branch.

4. JOINT FEATURE TRACKING

This section describes a vision processing method proposed for tracking variations in the geometry and location of the weld joint as the welding proceeds. However, extracting joint profile from the stripe images obtained during welding is far less

favorable than before the welding starts, because of the presence of tack welds and obstacles around the weld joint as well as the degradation of the stripe image data by arc glares and weld spatters radiating from the molten weld pool. Moreover, the time for the vision processing is required to be minimal to make the sensory feedback useful, whereas a relatively long time is allowed for the joint identification procedure. As one of the most promising methodologies to meet the requirements, a model-based pattern searching technique is adopted in this stage, which is based upon an elastic shape model technique followed by feature-based structure matching.

4.1. JOINT PROFILE SEARCHING: ACTIVE CONTOUR MODEL

The adopted active shape model, which is a modified version of active contour model originally developed by Kass *et al.* [13], is a method for finding a contour (closed or open curve), which corresponds to local minima of energy functional as shown by

$$E_{contour} = \int_0^1 [E_{internal}(r(s)) + E_{image}(r(s))] ds \quad (2)$$

where S is the arc length, and $r(s) = p(s) - q(s)$ denotes the relative distance vector of a point p on an elastic contour with respect to an anchor point q on a rigid core, as shown in Fig. 3. The basic goal of the model is to find a target contour of approximately known shape and pose from a given image. In the above representation, the rigid core represents the expectation on the shape and pose of the targeted contour to be extracted, and the elastic contour is a current estimation of the target contour. Fig. 3 illustrates an elastic shape model for searching a lap joint profile of approximately known shape and pose.

In the energy functional, E_{int} represents the internal energy of the model due to the prior shape constraints of the estimated elastic contour with respect to the rigid core. The internal model energy is written as

$$E_{internal} = (\alpha(s) |r_s(s)|^2 + \beta(s) |r_{ss}(s)|^2) / 2 \quad (3)$$

The contour energy is composed of the first-order term controlled by $\alpha(s)$ and the second-order term controlled by $\beta(s)$, in which the $\alpha(s)$ and $\beta(s)$ are weighting factors. The first-order term constraints the elastic contour to keep its own desired shape characterized by the rigid core and the second-order term prevents the elastic contour from abruptly deforming against the desired shape. The relative sizes of $\alpha(s)$ and $\beta(s)$ can be chosen to control the influence of the corresponding constraints on the internal energy.

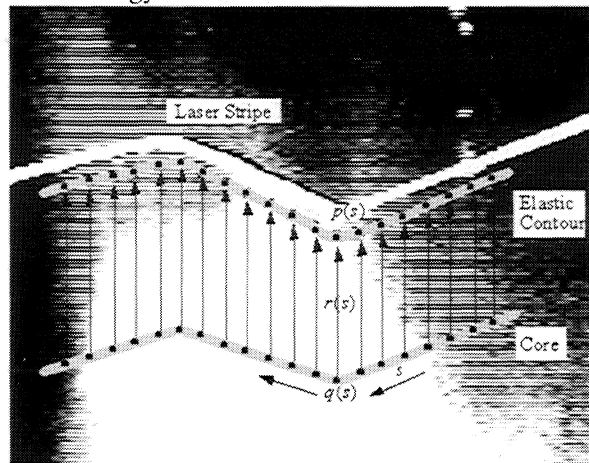


Fig. 3. Active contour model for searching the laser stripe in the typical lap joint image with the arc turned on

The image energy E_{image} is externally caused from image features. The goal is to push an estimated contour onto the main part of the laser stripe depicting the joint profile. There are some points, which should be considered for determining suitable image energy. The primary one is that the contour should be prevented from being pushed toward some other brightness sources, such as arc glares and welding spatters and so on. The other is that the image force should have a zero-crossing point in the center position of the cross-section of laser stripe: It means that the peak of the external image energy should appear in the center position of the cross-section. Consequently, we define an external image energy, which can be written as a form of

$$E_{image}(s) = -|G_{\sigma} * P(s)| \quad (4)$$

$$\text{where } P(s) = \begin{cases} R(s) & \text{if } R(s) > 0 \\ 0 & \text{otherwise} \end{cases}$$

In the expression, $R(s)$ is the response of the adaptive filter, as defined in Eq.(1), at the image coordinate $s(x, y)$, and G_{σ} is a Gaussian of the standard deviation σ .

The minimum energy contour can be determined using a variational method. The discretization of the associated Euler-Lagrange equation can be written in the following matrix form:

$$AR(t) + F_{image}(t) = 0 \quad (5)$$

where t is the time step, $R(t) = (r_1(t), r_2(t), \dots, r_N(t))^T$ is the radial distance vectors at the time t , and $F_{image}(t) = (f_{image,1}(t), f_{image,2}(t), \dots, f_{image,N}(t))^T$ is the external image forces. Here, $f_{image} = \nabla_r E_{image}$ is the first derivative of the image energy with respect to the radial distance vector. The number of control points N is chosen in accordance with the tradeoff between the search accuracy and the processing time. In the equation, the matrix A , called the stiffness matrix, represents all internal elastic relations of the shape model. The above equation can be numerically solved by using an implicit scheme for the term R and an explicit scheme for the term F_{ext} [18]. The result is obtained by

$$R(t) = D^{-1}B(t-1) \quad (6)$$

where the following identities are used:

$$D = \tau I + A \quad \text{and} \quad B(t-1) = \tau R(t-1) - F_{ext}(t-1) \quad (7)$$

Here, τ is a step size, which controls the convergence characteristics of the solutions with respect to time. As Eq.(6) evolves over time, an elastic contour placed near a target contour will move and deform toward the target contour. When the contour becomes stationary, a minimum energy contour will be obtained and it will fit the main part of the laser stripe (see [18] for more detailed explanation).

There still remains a problem for the elastic model to be used for automatically tracking variations in the joint profile as the welding proceeds. It is an initialization of the elastic contour and the rigid core because the elastic shape model assumes that a greater part of the initial elastic contour is placed closely to the target contour and the shape and pose of the core are close to those of the target contour. However, the initialization can be simply done on the basis of the joint profile previously identified. It needs only one step that is to place the well-shaped core and elastic contour on the identified stripe profile. In this case, the magnitude of all the radial distance vectors initially becomes zero. Meanwhile, the direction of all the radial distance vectors can be fixed to be parallel to the column direction of the image plane, because it can be assumed that a greater part of the laser stripe keeps being posed at relatively low angle with respect to the rows of the image during welding. Once the core and the elastic contour are initialized, the rest tracking is automatically performed by regarding the converged contour at the previous image as an initial contour for consecutive searching in the next incoming image.

The rigidity coefficients of the model, α and β , play an important role in the convergence process of the contour toward the targeted laser stripe. These coefficients should be chosen in such a correct way that the internal forces generated by the internal energy have the same magnitude as the external image forces. If the internal energy is predominant, the contour will be hard to adapt itself to variations in the geometry of the weld joint, whereas if the external energy predominates, the contour will tend to be trapped in the local areas with some fictitious image features due to arc glares, welding spatters or the secondarily reflected laser stripe from specular weld surface.

4.2. JOINT FEATURE DETECTION: FEATURE-BASED STRUCTURE MATCHING

Once the stripe profile is extracted, the next step is to find a list of significant structural features of the weld joint. First of all, the break points located at the significant orientation changes along the profile are obtained from the list of the straight line segments fitted to the original profile. The least square fitting or the polygon approximation techniques can be used for obtaining the fitted line segments. Detection of the joint features is based on the feature-based template matching. The goal is to find the best match of the extracted breakpoints with the template previously constructed, where the best match is found when the template is attached to the breakpoints such that the total matching cost is minimized.

Suppose that the i^{th} branch of the template profile is matched to the breakpoints b_q and b_r of the input profile (see Fig. 4). In this case, the matching cost $C_i(q,r)$ is defined by

$$C_i(q,r) = w_l L_i(q,r) + w_a A_i(q,r) + w_s S_i(q,r) \quad (8)$$

where w_l , w_a and w_s are weighting factors, and $L_i(q,r)$, $A_i(q,r)$ and $S_i(q,r)$ denote the measures of similarity in length, angle and straightness between the pair to be considered for matching, respectively. The measures are given by

$$L_i(q,r) = \left| \frac{l_i - D(b_q, b_r)}{l_i} \right|, \quad (9)$$

$$A_i(q,r) = \left| \frac{\theta_i - \angle(b_q, b_r)}{90} \right|,$$

$$\text{and } S_i(q,r) = \left| 1 - \frac{D(b_q, b_r)}{G(b_q, b_r)} \right|$$

where $D(b_q, b_r)$ is the distance between breakpoints b_q and b_r , and $\angle(b_q, b_r)$ denotes the angle of a artificial line passing through these two points with respect to the rows of the image. Also, $G(b_q, b_r)$ is the sum of all the distances between two consecutive breakpoints existing between the points b_q and b_r . The straightness similarity suggests that, as a proper matching candidate, a single line segment is preferred than an artificial line segment combining multiple line segments having different angles from each other. The total matching cost C is the sum of each the matching cost over all the branches comprising the template profile. If the total matching cost at the best match is smaller than a threshold value, the matched breakpoints serve to determine the joint features. And, the attributes of the template are newly replaced with the detected joint features to cope with some possible variations of the joint geometry in the next incoming image. If the match cost is larger than the threshold value, the feedback to the welding robot is bypassed.

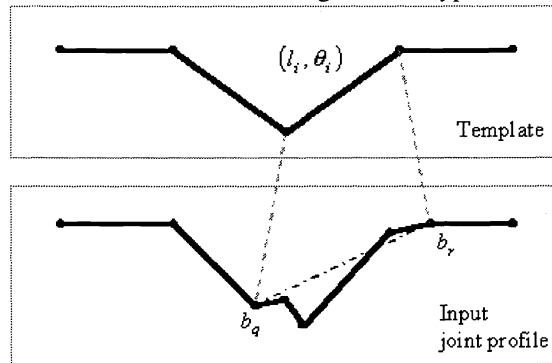


Fig. 4. Feature-based template matching

5. EXPERIMENTAL RESULTS AND DISCUSSIONS

To investigate the performance of the developed algorithm, a series of tests have been carried out by using the actual robotic welding system. In each welding experiments, the gas metal arc (GMA) welding has been processed on the workpieces of the hot rolled steel 1025.

5.1. JOINT FEATURE DETECTION

Fig. 5 shows the joint structure identification results obtained by using the syntactic analysis. The top images show a list of the line segments resulted from the polygon approximation conducted on the laser stripe data extracted by the adaptive filter from three different joint images. In the figures, small rectangles mark the endpoints of each the line segments. The below images depict the finally identified joint structures. The results show that all of the inherent joint structures were successfully identified regardless of the presence of many overrefined, missing or artificial segments. More experimental results on joint identification are given in the previous work [19].

In all of the results, the following parameters have been used: $D_{th} = 6$, $U_{th} = 15$, $V_{th} = 10$, and $P_{th} = 20$. From a number of

experiments with different parameters, it appeared that choice of parameter P_{th} was most critical to the results. If the value is too small, a number of artificial features are generated. This often caused incorrect identification of joint structure. In the case of lap, fillet and vee joints, the excessively large values also led to incorrect identification because it prevented the detection of relevant features. The values of thresholds D_{th} , U_{th} and V_{th} need to be varied according to particular geometry of the workpieces to be welded, such as gap size or material thickness.

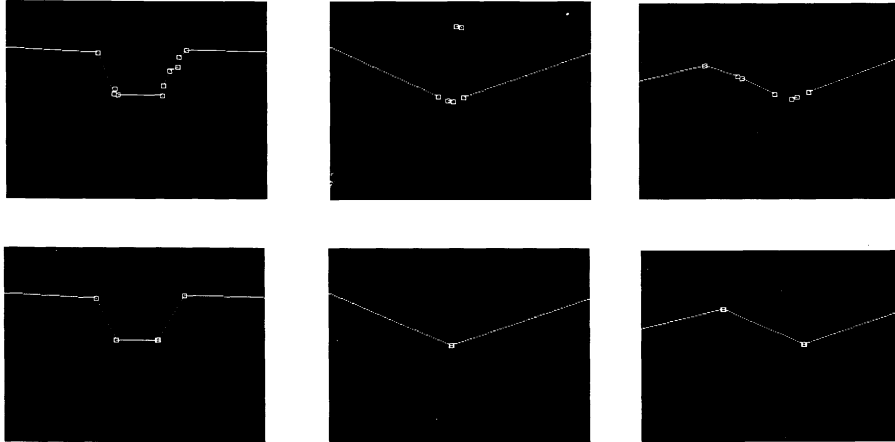


Fig. 5. Joint structure identification using syntactic analysis

Figs. 6 and 7 show the successive tracking results of joint features from the stripe images with the arc turned on, which possess intensive optical noises, such as arc glares and weld spatters. In each figures, the stripe images are overlaid by an elastic contour. Each of the figures (a) show the initial elastic contour, which, in fact, was borrowed from the contour at the equilibrium state of the previous processing time. Figs. 6(b) and (c) and Fig. 7(b) show the elastic contours at the intermediate state. The rest images exhibit the final contour converged to the steady state, where small rectangles on the contour marks the joint features finally resulted from the template matching. From the results, it can be shown that variations in the pose and geometry of the weld joint can be successfully tracked regardless of the presence of intensive arc glares and weld spatters covering wide area around the weld joint.

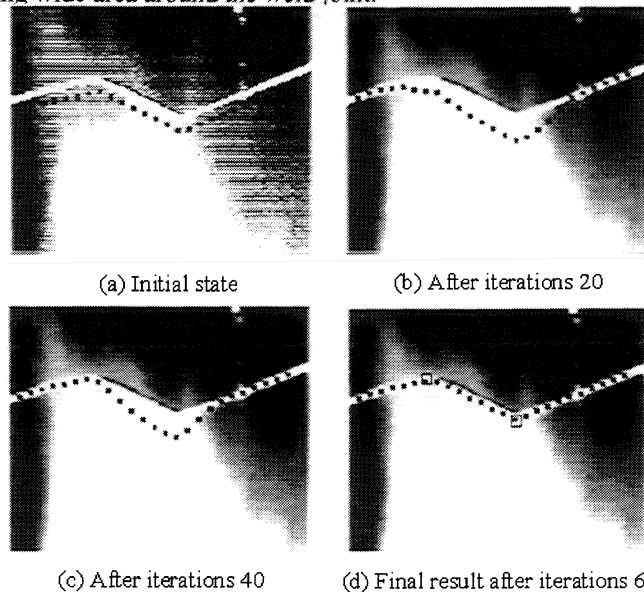


Fig. 6. Joint feature tracking result in case the torch is approaching to weld joint surface as the welding proceeds: lap joint

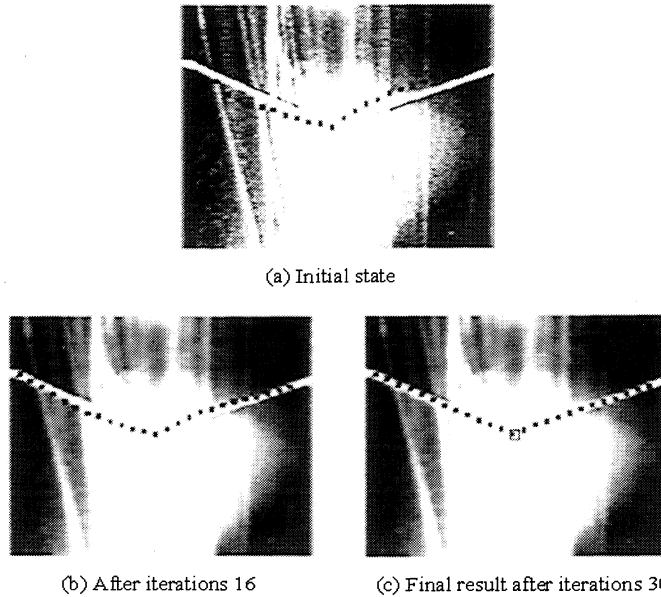
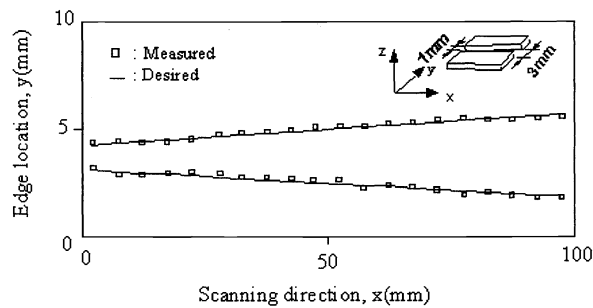


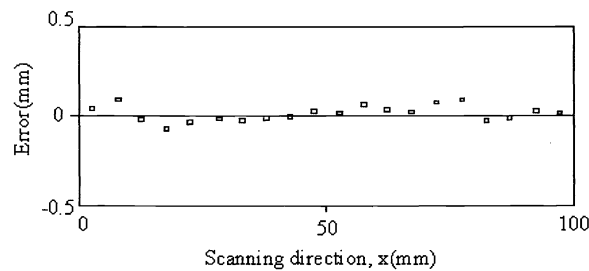
Fig. 7. Joint feature tracking result in case the torch is slanting against its current pose as the welding proceeds: fillet joint

5.2. ROBOTIC JOINT TRACKING

Once the joint features are located in the image plane, the three-dimensional geometry of the weld joint needs to be determined to guide the welding torch path. The three-dimensional geometry can be obtained with the vision sensor model. In this work, the vision sensor model was off-line obtained by using an accurately machined block of known dimensions according to the standard linear least squares fit technique as described in Ballard et al. [20].



(a) Desired vs. measured edge location



(b) Measurement error

Fig. 8. Measurement result of gap size in butt joint

To evaluate the measurement accuracy of the joint features, tests have been performed on a variety of weld joints of different sizes. One of the results is the measurement of gap size in butt joint, as shown in Fig. 8. In (a) of the figure, two straight solid lines represent actual locations of butt joint edges, whereas the measured locations are remarked by small rectangles. The measurement errors in gap size are shown in the figure (b). The results exhibit that the measurement errors

always occur below $\pm 0.2\text{mm}$. It is obvious that these measurement errors include both errors in the vision sensor modeling and vision processing.

To test the seam tracking ability by the developed scheme, a number of robotic arc weldings guided by the vision processing results have been conducted on various weld joint types. One of the results is shown in Fig. 9 and 10 in which the butt joint of curved shape on the flat plates ($300\text{mm} \times 220\text{mm} \times 8\text{mm}$) slanted upwards along the welding direction was used. The vision sensor was located ahead of the torch by a distance of 35mm and the welding input power was increased to 4300W. The two results quantitatively evaluate the degree of the influence of the optical noises on the seam tracking accuracy by comparing the torch positions with the arc turned off with those with the arc turned on. In this figures, x axis is aligned with the welding direction, while z axis represents the height of the torch with respect to the workpiece coordinates. Fig. 9 shows the torch paths in the x - y plane, whereas Fig. 10 in the x - z plane. In (b) of these figures, the results show that additional distortion of the torch position by the welding noises added during welding is always below $\pm 0.1\text{mm}$ and so we can conclude that the tracking accuracy by the proposed scheme is little influenced by the level of the added optical noises.

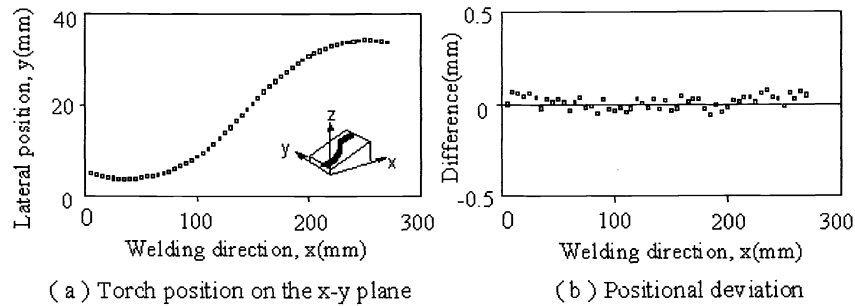


Fig. 9. Comparison of vision-guided seam tracking results in the x - y plane: arc on versus arc off

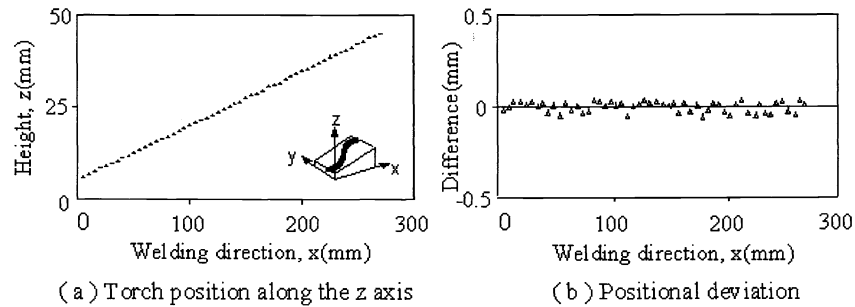


Fig. 10. Comparison of vision-guided seam tracking results in the x - z plane: arc on versus arc off

6. CONCLUSIONS

This paper dealt with a vision processing scheme for adaptive seam tracking in arc welding process. Significant effort was directed in the development of the vision algorithm with robustness to hostile welding environments. Basic idea underlying the method lies in a model-based pattern search, which is based upon an active shape model technique following feature-based structure matching.

The developed vision processing scheme showed several distinct features. Most distinct feature is the robustness of the algorithm against various optical noises induced during welding, which mainly owes its origin to the active shape model technique. The second is the generality of the algorithm. Although the algorithm in the present form dealt with only the typical four joint types, it can be easily extended to treat other joint types by simply adding new pattern primitives to the shape vocabulary. The third lies in its autonomy. It does not need any external information on the weld joint to be welded to perform the joint identification and tracking. The other is its efficiency in the viewpoint of the computation time. Accordingly, the algorithm could supply the measured joint geometric data at a rate of about 2-3 times per second although most part of the algorithm ran on the Intel 80486 processor. Nevertheless, more successful practical implementation of the algorithm will depend on the availability of faster processors.

REFERENCES

- [1] M. Kawahara, "Tracking control system using image sensor for arc welding," *Automatica*, Vol.19, pp.357-363, 1983.
- [2] Z. Smati, D. Yapp and C.J. Smith, "Laser guidance system for robots," *Proc. 4th Int. Conf. on Robot Vision and Sensory Controls*, pp.91-101, 1984.
- [3] R.W. Richardson, R.A. Gutow, R.A. Anderson and D.F. Farson, "Coaxial arc weld pool viewing for process monitoring and control," *Welding Journal*, Vol.63, pp.43-50, 1984.
- [4] W.F. Clocksin, J.S.E. Bromley, P.G. Davey, A.R. Vidler and C.G. Morgan, "An implementation of model-based visual feedback for robot arc welding of thin sheet steel," *Int. J. of Robotics Research*, Vol.4, pp.13-26, 1985.
- [5] J.E. Agapakis, "Visual sensing and knowledge-based processing for automated robotic welding fabrication." *Proc. Int. Computers in Engineering Conf.*, Vol.1, pp.225-231, 1985.
- [6] N. Nayak, D. Thompson, A. Ray and A. Vavrek, "Conceptual development of an adaptive real-time seam tracker for welding automation," *Proc. 1987 IEEE Int. Conf. on Robotics and Automation*, pp.1019-1024, 1987.
- [7] H.H. Kim, A vision system for real-time weld seam tracking in arc welding processes. M.S. Thesis, KAIST, Korea, 1989.
- [8] P. Sicard and M.D. Levine, "Joint recognition and tracking for robotic arc welding," *IEEE Trans. on Systems, Man, and Cybernetics*. Vol.19, pp.714-728, 1989.
- [9] J.E. Agapakis, "Approaches for recognition and interpretation of workpiece surface features using structured lighting," *Int. J. of Robotics Research*, Vol.9, pp.3-16, 1990.
- [10] J.E. Agapakis, J.M. Katz, J.M. Friedman and G.N. Epstein, "Vision-aided robotic welding : An approach and a flexible implementation," *Int. J. of Robotics Research*, Vol.9, pp.17-34, 1990.
- [11] Yoshinori Kusachi, Koichi Kato, Masashi Okudaria, "Tracking a feature point in profile data using an articulated object model and tuning parameters using the genetic algorithm", *Proc. of 1999 7th IEEE International Conference on Engineering Technologies and Factory Automation*, Vol.1, pp.145-150, 1999
- [12] Karsten Haug and Gunter Pritschow, "Reducing distortions caused by the welding arc in a laser stripe sensor system for automated seam tracking", *Proc. of the IEEE International Symposium on Industrial Electronics*, Vol.2, pp.919-924, 1999
- [13] M. Kass, A. Witkin and D. Terzopoulos, "Snake: Active contour models," *Int. Journal of Computer Vision*, pp.321-331, 1988.
- [14] K. Inoue, "Image processing for on-line detection of welding process (Report 3) - Improvement of image quality by incorporation of spectrum of arc," *Transactions of JWRI*, Vol.10, pp.13-18, 1981.
- [15] R.J. Popplestone and A.P. Ambler, *Forming body models from range data*. Research Report 46, Department of Artificial Intelligence, University of Edinburgh, 1977.
- [16] T. Pavlidis and S.L. Horowitz, "Segmentation of plane curves," *IEEE Trans. Comput.*, Vol.23, pp.860-870, 1974.
- [17] J.S. Kim, Y.T. Son, H.S. Cho and K.I. Koh, "A robust visual seam tracking system for robotic arc welding," *Mechatronics*, to appear.
- [18] J.S. Kim, K.C. Koh and H.S. Cho, "An active contour model with shape regulation scheme", *Advanced Robotics*, to appear, 2000.
- [19] J.S. Kim, Y.T. Son, H.S. Cho and K.I. Koh, "A robust method for vision-base seam tracking in robotic arc welding," *IEEE Int. Symposium on Intelligent Control*, Florida, USA, 1995.
- [20] D.H. Ballard and C.M. Brown, *Computer vision*. Prentice Hall, Englewood Cliffs, NJ, 1982.